High Molar Extinction Coefficient Branchlike Organic Dyes Containing Di(p-tolyl)phenylamine Donor for Dye-Sensitized Solar Cells Applications

ARTICLE *in* THE JOURNAL OF PHYSICAL CHEMISTRY C · FEBRUARY 2010

Impact Factor: 4.77 · DOI: 10.1021/jp911139x

High Molar Extinction Coefficient Branchlike Organic Dyes Containing Di(*p*-tolyl)phenylamine Donor for Dye-Sensitized Solar Cells Applications

Huajie Chen,[†] Hui Huang,[†] Xianwei Huang,[†] John N. Clifford,[‡] Amparo Forneli,[‡] Emilio Palomares,[‡,§] Xiaoyan Zheng,[†] Liping Zheng,[†] Xianyou Wang,[†] Ping Shen,[†] Bin Zhao,[†] and Songting Tan*[,†]

College of Chemistry, and Key Laboratory of Advanced Functional Polymeric Materials, College of Hunan Province, and Key Laboratory of Environmentally Friendly Chemistry and Applications of Ministry of Education, Xiangtan University, Xiangtan 411105, P. R. China, Institute of Chemical Research of Catalonia (ICIQ), and Avinguda PaÏsos Catalans, 16 Tarragona 43007, Spain, and Catalan Institution for Research and Advanced Studies (ICREA), Spain

Received: September 23, 2009; Revised Manuscript Received: January 9, 2010

Two novel branchlike organic dyes (**D1** and **D2**) comprising two di(*p*-toyl)phenylamine moieties as the electron donor, cyanoacetic acid moieties as the electron acceptor, thiophene or 3-hexylthiophene moieties as the Π-spacer, were designed and synthesized for dye-sensitized solar cells (DSSCs). It was found that the introduction of two di(*p*-tolyl)phenylamine groups to form the branchlike configuration exhibited better photovoltaic performance due to the improvement of the electron donating and the light-harvesting properties. By the introduction of two di(*p*-tolyl)phenylamine groups into the framework of **D2**, it is interesting to note that the UV−vis absorption of **D2** showed an obvious blue-shift but also improved molar extinction coefficient compared with that of **D3**. The transient absorption measurements showed that the dyes **D1** and **D2** with two di(*p*-tolyl)phenylamine-substitutes could effectively retard charge recombination between electrons at the TiO_2 and the oxidized dyes. Among the three dyes studied, a maximum power conversion efficiency of 6.41% was obtained under simulated AM 1.5 G solar irradiation (100 mW/cm^2) with a DSSC based on **D2** dye (J_{sc} = 11.62 mA/cm^2, V_{oc} = 0.73 V, FF = 0.756) upon the addition of 1.0×10^{-3} M chenodeoxycholic acid (CDCA) as coadsorbent.

Introduction

Increasing energy demands and concerns over global warming have led to a great focus on renewable energy sources in recent years. Dye-sensitized solar cells (DSSCs) are regarded as low cost next-generation solar cells. Great progress has been made in their performance and stability since the pioneering study by O'Regan and Grätzel in 1991.[1] The performances of the DSSCs are mainly affected by the photosensitizer, the anode, the cathode and the electrolyte.[2] Among the factors that affect drastically the device power conversion efficiency, the dyes play a key role for the DSSCs to obtain high power conversion efficiency (η) and have been intensively studied by researchers worldwide. Until now, several Ru(II) polypyridyl complexes, such as **C101**, have achieved a record η above 11% under standard solar illumination (global air mass 1.5).[3] Although the most efficient sensitizers to date are ruthenium complexes, the high cost and stability issues still limit the large-scale application of this type solar cells.

In order to obtain even cheaper photosensitizers for DSSCs, metal-free organic dyes have also been attracting intensive research efforts because they have many advantages such as their high molar extinction coefficient, facile modification for tunable absorption spectral response, and they are more environment friendly. In the past decades, various dipolar metal-free dyes such as coumarin,[4] indoline,[5] oligoene,[6] merocyanine,[7] hemicyanine,[8] porphyrin,[9] triarylamine,[10] and carbazole[11] dyes have been reported as photosensitive dyes. Among these dyes, an impressively high efficiency of 9% has been achieved for DSSCs based on an indoline organic dye[5a] even though it has significantly shorter absorption wavelength as compared with **N719** dye. The high performance of this device can be attributed partly to the high molar extinction coefficient, 68 700 M^{-1} cm^{-1} at 526 nm.

To obtain optimal performance, charge recombination of conduction band electrons with triiodide, Π−Π* stacking and the formation of dye aggregates on the semiconductor surface also need to be avoided through appropriate structural modification or coadsorption of dyes with additives. Recently, Hsu et al[10d] reported that incorporation of double triphenylamine (TPA) moieties at 1*H*-phenanthro[9,10-*d*]imidazole was found to effectively retard charge recombination of the electrons in the TiO_2 and the oxidized dyes. In adition, Yang et al[10a] working with triphenylamine-based organic dyes, which tuned the TPA electron donor by substituting two methyl groups to improve the electron-donating ability and prevent unfavorable dye aggregation, obtained high power conversion efficiency of 7%. To the best of our knowledge, the high molar extinction coefficient branchlike metal-free organic dyes used as the photosensitizers of the DSSCs have not been reported.[12,10b,c]

Herein, we report the design and synthesis of two new branchlike di(*p*-tolyl)phenylamine/ cyanoacrylic acid dyes (**D1** and **D2**, shown in Figure 1). For comparison purposes, the dye **D3**, which has no double di(*p*-tolyl)phenylamine substitutes as the donor, was also synthesized. The double di(*p*-tolyl)phenylamine moieties were selected as the donor based on the

* Corresponding author. E-mail: tanst2008@163.com.
[†] Xiangtan University.
[‡] ICIQ.
[§] ICREA.

10.1021/jp911139x
Published on Web 02/02/2010

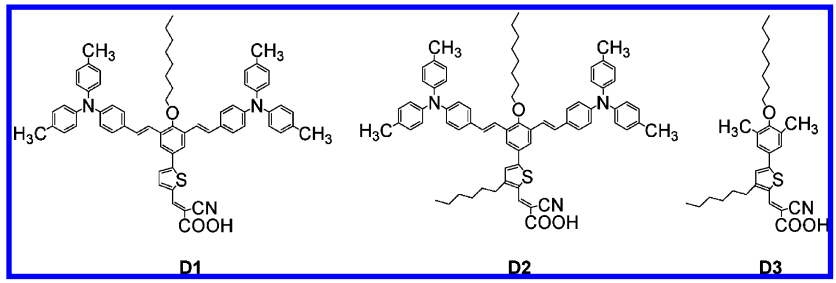

Figure 1. Molecular structures of the dyes **D1**, **D2**, and **D3**.

following reasons: (1) by incorporating electron donor TPA group into the dye molecules, the physical separation of the dye cation from the TiO_2 electrode surface will be increased, which efficiently retards recombination between the photoelectron and the oxidized dyes.[13] It is natural to assume that this effect will be further enhanced by introducing double di(*p*-tolyl)phenylamine moieties into the dye molecules. (2) Compared with one electron donor group, double di(*p*-tolyl)phenylamine moieties as the electron donors not only have much stronger electron-donating ability but also much more steric hindrance, which should strongly prevent unfavorable dye aggregation.[14,10a] In this article, we study the effects of the electron donor and with/ without a hexyl chain in the Π-spacer on the photophysical, photochemical, electrochemical properties, and power conversion efficiency. In particular, transient absorption spectroscopy was employed to monitor interfacial charge-recombination kinetics in dye sensitized TiO_2 films. To further improve the performances of the solar cells based on these dyes, CDCA as coadsorbent was added into the dye bath. Among these dyes, **D2** exhibited the highest power conversion efficiency of 6.41% under AM 1.5 irradiation with 100 mW/cm^2 simulated sunlight, indicating its potential application as the metal-free organic dyes in DSSCs.

Experimental Section

Analytical Measurements. ^{1}H and ^{13}C NMR spectra were recorded with a Bruker Avance 400 instrument. FT-IR, UV−vis spectra, and PL spectra were obtained on PE One Spectra, PE Lamada 25 spectrometer, and PE LS-50 luminescence spectrometer, respectively. MALDI-TOF mass spectrometric measurements were performed on Bruker AutoFlex III MALDI-TOF. Electrochemical redox potentials were obtained by cyclic voltammetry (CV) using a three-electrode configuration and an electrochemistry workstation (CHI660A, Chenhua Shanghai). The working electrode was a glassy carbon electrode; the auxiliary electrode was a Pt electrode, and saturated calomel electrode (SCE) was used as reference electrode. Tetrabutylammonium perchlorate (TBAP) 0.1 M was used as supporting electrolyte in dry toluene/acetonitrile ($v/v = 8/2$). Ferrocene was added to each sample solution at the end of the experiments, and was used as an internal potential reference.[15] Transient absorption spectroscopy was carried out with a system consisting of a nitrogen laser with tunable excitation wavelength. The sample is positioned between two monochromators and a 150 W tungsten lamp is used as light probe. A Costronics silicon detector connected to a Tektronic oscilloscope TDS 2022 and to an electronic filter box is used to monitor the change in absorbance after the laser pulse excitation.

General Procedure for Preparation and Test of Solar Cells. The FTO glass (fluorine doped SnO_2, sheet resistance 14 Ω/sq, transmission >90% in the visible) was first cleaned in a detergent solution using an ultrasonic bath for 15 min and then rinsed with water and ethanol. The washed FTO glass was immersed in 40 mM aqueous $TiCl_4$ solution at 70 °C for 30 min and then washed with water and ethanol. Titania paste was prepared from 12 g of P25 (Degussa AG, Germany) following a literature procedure[16] and added with 3.6 mL of 1% magnesium acetate solution.[17] Then the paste was deposited onto the FTO glass by sliding glass rod method. The TiO_2-coated FTO glass was sintered at 450 °C for 30 min in air. The sintered film was treated with 40 mM $TiCl_4$ aqueous solution at 70 °C for 30 min and annealed again at 450 °C for 30 min. After the film was cooled to 80 °C, it was immersed into 1.0×10^{-3} M dye of toluene solution with/without 1.0×10^{-3} M CDCA[18] and maintained under dark overnight. The electrode was then rinsed with toluene and dried. One drop of electrolyte solution was deposited onto the surface of the electrode and penetrated inside the TiO_2 film via capillary action. The electrolyte consists of 0.5 M LiI, 0.05 M I_2, and 0.5 M 4-*tert*-butylpyridine (TBP) in 3-methoxypropionitrile. A Pt foil used as counter electrode was clipped onto the top of the TiO_2 working electrode. The photocurrent−voltage (*J-V*) characteristics were recorded on Keithley 2602 Source meter under 100 mW/cm^2 simulated air mass (AM 1.5) solar light illumination. The action spectra of monochromatic incident phototo-current conversion efficiencies (IPCEs) for the solar cells were also detected with a similar data acquisition system. Light from the Xe lamp was focused through a monochromator onto the photovoltaic cell.

Results and Discussion

Synthesis of the Materials. The structures and synthetic routes of the three dyes are shown in Figure 1 and Scheme 1, respectively. All of the dyes have been synthesized according to several classical reactions, and detailed synthetic procedures are described in the Supporting Information. The starting material, 3-hexylthiophene-2-carbaldehyde, was synthesized from 2-bromo-3-hexylthiophene in the presence of Mg and DMF using the method as described by Demandrille et al.[19] The key intermediate of compound **3** was obtained through two steps: (1) the aldehyde function of thiophene-2-carbaldehyde was protected by a conversion into the glycol acetal, obtaining the corresponding compound **1**, and (2) the compound **1** was converted into compound **3** in the presence of n-BuLi and tributyltin chloride. The synthetic procedure for compound **4** was similar to that for compound **3** except that 3-hexylthiophene-2-carbaldehyde was used instead of thiophene-2-carbaldehyde. Another key intermediate, *N*-(4-((1E,7E)-3-((*E*)-4-(di-*p*-tolylamino)styryl)-5-bromo-2-(octyloxy)styryl)phenyl)-4-methyl-N-*p*-tolylbenzenamine **8**, was obtained in high yield by using 5-bromo-1,3-bis(diethyl-phsophonate-methyl)-2-(octyloxy)benzene **7** and an excess 4-(di-*p*-tolylamino)benzaldehyde in the Wittig−Horner reaction. Then the compound **8** was coupled with compound **3** or **4** through the Stille coupling reaction to obtain compound **9** or **10**. The synthetic procedure

SCHEME 1: Synthetic Routes to Three Dyes[a]

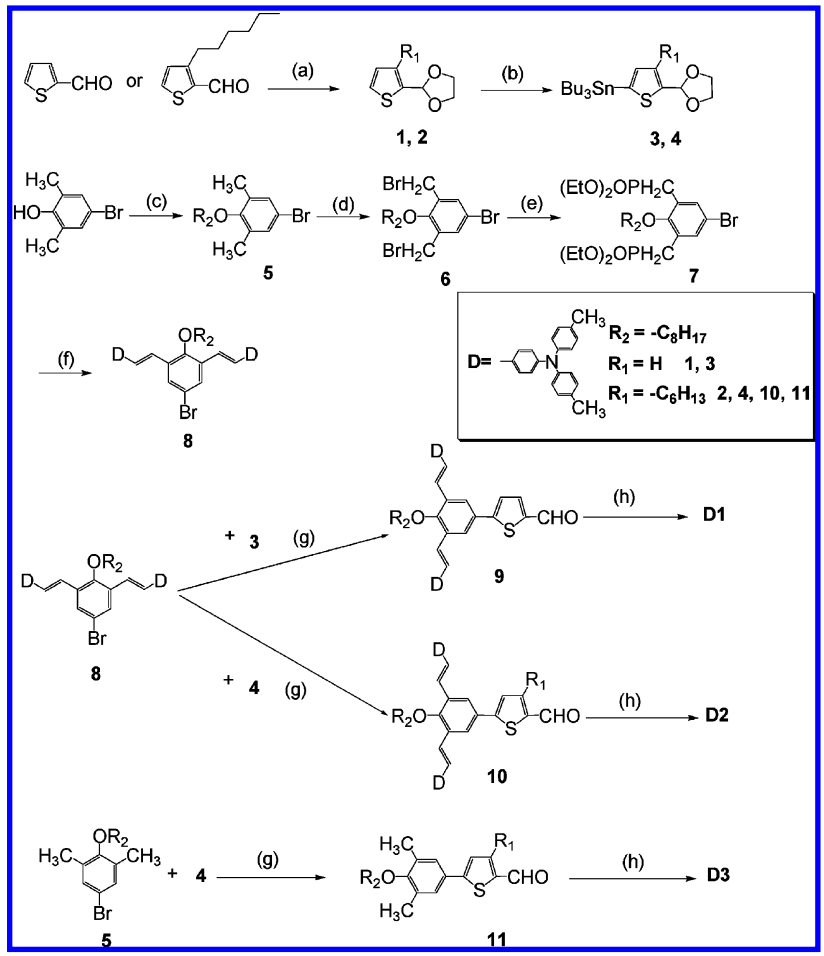

[a] Reagents and conditions: (a) benzene, glycol, *p*-toluenesulfonic acid. (b) (i) THF, n-BuLi, −78 °C; (ii) Bu_3SnCl, −78 °C. (c) DMF, $C_8H_{17}Br$, K_2CO_3. (d) CCl_4, NBS. (e) Triethyl phosphtie, 160 °C. (f) THF, 4-(di-*p*-tolylamino)benzaldehyde, *t*-BuOK. (g) (i) DMF, $Pd(PPh_3)_4$; (ii) HCL, H_2O. (h) $MeCN/HCCl_3$, cyanoacetic acid, piperidine.

TABLE 1: Maximum Absorption and Emission Data of the Three Dyes

dye	λ_{abs}/nm (ε/M^{-1} cm^{-1})[a]	λ_{max}/nm[b] (on TiO_2)	λ_{ex}[c] (nm)
D1	400 89 000	410	471
D2	401 74 000	411	472
D3	413 21 000	425	502

[a] Maximum absorption in $CHCl_3$ solution (1.0×10^{-5} M) at 25 °C. [b] Maximum absorption on TiO_2 film. [c] Maximum emission of the dyes in $CHCl_3$ solution (1.0×10^{-5} M) at 25 °C. ε is the molar extinction coefficient at ν_{abs} of maximum absorption.

for compound **11** was similar to that for compound **10** except that compound **5** was used instead of compound **8**. Subsequently, the Knoevenagel condensation reactions of aldehyde derivatives **9**∼**11** with cyanoacetic acid gave the target dyes **D1**∼**D3** in the presence of piperidine.

Optical Properties. Optical data and UV−vis spectra of the three dyes in $CHCl_3$ solution are provided in Table 1 and Figure 2, respectively. **D1** and **D2** exhibit a strong absorption maximum in the visible region (400−415 nm) corresponding to the intramolecular charge transfer (ICT)[20] between the di(*p*-tolyl)phenylamine donor and the cyanoacetic acid acceptor and a relatively weak shoulder in the near-UV region (280−310 nm) due to the π-π^* electron transitions of the conjugated molecules. The spectra of **D1** and **D2** are quite similar, but the molar extinction coefficient of **D2** (ε = 74 000 M^{-1} cm^{-1} at 400 nm) is smaller than that of **D1** (89 000 M^{-1} cm^{-1} at 401

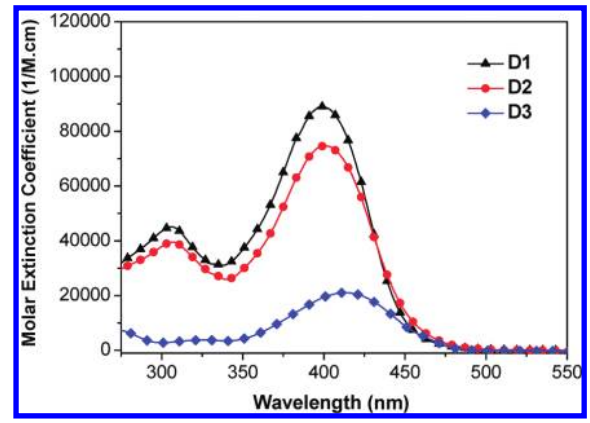

Figure 2. Absorption spectra of the three dyes in $CHCl_3$ solutions (1.0×10^{-5} M).

nm), which can be attributed to the introduction of the hexyl-substitute into Π-conjugated thiophene-birdge in the former.[11] When two di(*p*-tolyl)phenylamine groups were introduced into the framework of **D1** and **D2** to form the branchlike configuration, the absorption maxima of **D1** and **D2** show slight blue-shift compared with that of **D3** (see Table 1). This blue-shifted phenomenon can be readily understood from molecular modeling studies (Figure 3). The ground-state structures of **D1**∼**D3** have twist angles of 28.4°, 30.3° and 0°, respectively, between thiophene or 3-hexylthiophene and the adjacent benzene units.

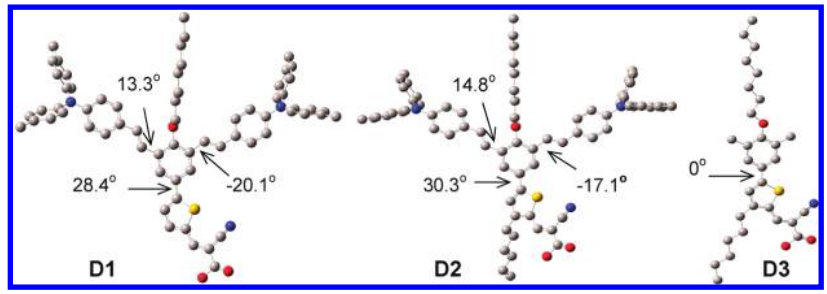

Figure 3. Optimized structures calculated by TD-DFT using the B3LYP functional and the 3-21G* bases set for **D1**, **D2**, and **D3**.

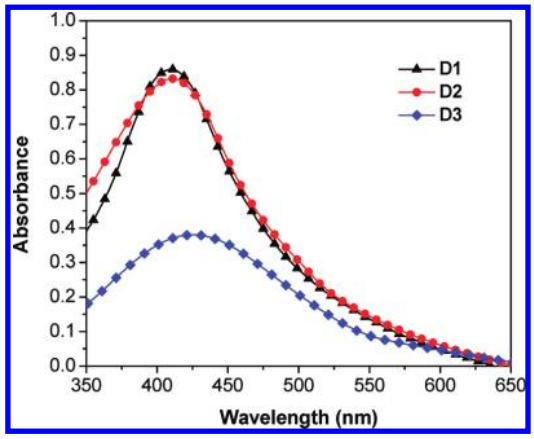

Figure 4. Absorption spectra of the three dyes adsorbed on TiO_2 films.

Besides, the dihedral angles of the vinylene-benzene bridged units are 13.3° and −20.1° for **D1** and 14.8° and −17.1° for **D2**, respectively. These results indicate that **D3** has a more coplanar geometry, but **D1** and **D2** have a twisted nonplanar geometry due to the introduction of large bulk groups of double di(*p*-toyl)phenylamine donors. In addition, the molar extinction coefficients of **D1** (ε = 89 000 M^{-1} cm^{-1} at 400 nm) and **D2** (ε = 74 000 M^{-1} cm^{-1} at 401 nm) are much higher compared with that of **D3** (21 000 M^{-1} cm^{-1} at 413 nm), which might be attributed to the ICT between the di(*p*-tolyl)phenylamine donor and the cyanoacetic acid acceptor and the π-π* electron transitions of the conjugated molecules. This result indicates that the presence of di(*p*-tolyl)phenylamine-substitutes in a dye significantly increases the light harvesting efficiency.

Figure 4 shows the absorption spectra of the three dyes adsorbed on the TiO_2 films, and the corresponding data are collected in Table 1. We can see that the maximum absorption peaks (λ_{max}) for the three dyes are similar to the corresponding solution spectra but exhibit a small red shift about 10−12 nm due to the interaction of the anchoring groups with the surface titanium ions. The amounts of the adsorbed dyes on the TiO_2 films were estimated by desorbing the dyes with basic solution, and the surface concentrations were determined to be 4.16 × 10^{-8}, 3.38 × 10^{-8}, and 3.14 × 10^{-8} mol cm^{-2} for **D1**-, **D2**-, and **D3**-sensitized films, respectively. It is important to note that the adsorbed dye density is similar in different TiO_2 films, and the influence of dye density on the cell performances can be considered unimportant in our later discussion.

Figure S1 (see the Supporting Information) shows the emission spectra of the three dyes in $CHCl_3$ solution (1.0 × 10^{-5} M). The corresponding data are also summarized in Table 1. From the Figure S1, we can see that the maximum emission wavelength in $CHCl_3$ solution is in the order of **D3** > **D2**∼**D1**, which is consistent with that of the maximum absorption in $CHCl_3$ solution. Comparing **D1** and **D2** with **D3**, the maximum emission wavelength shows a blue shift due to the introduction of the two di(*p*-tolyl)phenylamine-substitutes into **D3** (502 nm for **D3**).

TABLE 2: Electrochemical Data of the Three Dyes[a]

dye	λ_{int}/nm	E_{0-0}/eV	$E(s^+/s)$/V vs NHE	$E(s^+/s^*)$/V vs NHE	E_{gap}/V
D1	440	2.82	1.07	−1.75	1.25
D2	442	2.81	1.02	−1.79	1.29
D3	454	2.73	1.20	−1.53	1.03

[a] E_{0-0} values were calculated from intersection of the normalized absorption and the emission spectra (λ_{int}): E_{0-0} = 1240/λ_{int}. The ground-state oxidation potential (vs NHE), $E(s^+/s)$, was measured in toluene and acetonitrile (v/v = 8/2) and calibrated by addition of 0.63 V to the potential versus Fc/ Fc^+. The excited-state oxidation potential, $E(s^+/s^*)$, was calculated from $E(s^+/s)$ − E_{0-0}. E_{gap} is the energy gap between the $E(s^+/s^*)$ of dye and the conduction band level of TiO_2 (−0.5 V vs NHE).

Electrochemical Properties. To evaluate the possibility of electron transfer from the excited dye molecule to the conductive band of TiO_2 and the dye regeneration, cyclic voltammetry (CV) method was employed in toluene and acetonitrile (v/v = 8/2) solution, using tetrabutylammonium perchlorate (TBAP) as a supporting electrolyte, and the data are summarized in Table 2. The ground-state oxidation potentials ($E(s^+/s)$ vs NHE) correspond to the HOMO levels of the dyes, ranging from 1.02 to 1.20 V vs NHE, are all more positive than the iodide/ triiodide redox couple (∼0.42 V vs NHE), ensuring that there is enough driving force for efficient regeneration of the dye through the recapture of the injected electrons by the dye cation radical. Comparing **D2** with **D3**, the HOMO value of **D2** shifted in a negative direction due to introduction of two di(*p*-tolyl)phenylamine donors. The same phenomenon was observed by comparing **D2** with **D1**. Namely, a hexyl-substitute was introduced into the framework of **D2**, the HOMO value of **D2** also resulted in a slight negative shift of 5 mV.

By neglecting any entropy change during light absorption, the excited-state oxidation potentials ($E(s^+/s^*)$ vs NHE), which correspond to the LUMO levels of the three dyes, were calculated by $E(s^+/s)$ − E_{0-0}, where E_{0-0} is the zeroth−zeroth energy of the dyes which estimated from the intersection between the normalized absorption and emission spectra. The data are collected in Table 2. From the absorption and emission spectra, E_{0-0} energies of 2.82, 2.81, and 2.73 eV are extracted for **D1**, **D2**, and **D3**, respectively. The LUMO levels of the three dyes are more negative (−1.53 V vs NHE for **D3**) than that of the TiO_2 conduction band edge (−0.5 V vs NHE),[21] and the energy gap (E_{gap}) between the conduction band and the LUMO levels of dye increases from 1.03 V for **D3** to1.25 V for **D1** and then to 1.29 V for **D2**. By assumption that E_{gap} of 0.2 eV is necessary for efficient electron injection, so these driving forces are sufficiently large for effective electron injection.

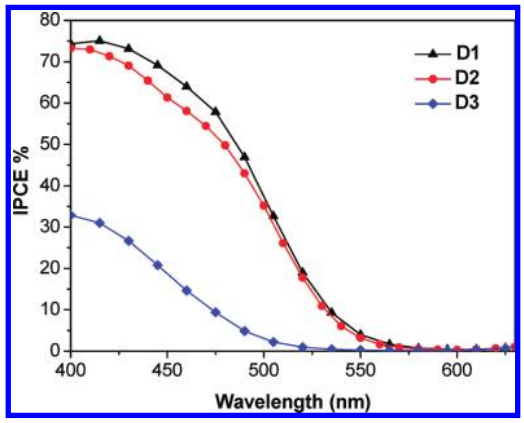

Figure 5. IPCE plots for the DSSCs based on the three dyes without CDCA as coadsorbent.

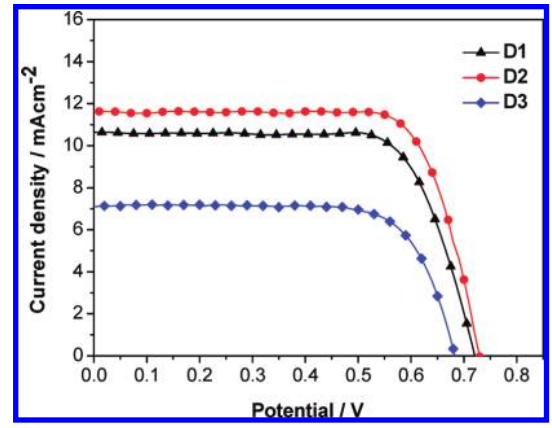

Figure 6. Current density−voltage characteristics for DSSCs based on the three dyes with CDCA (1.0×10^{-3} M) as coadsorbent.

TABLE 3: Photovoltaic Performance of DSSCs for the Three Dyes Based on Different Measured Conditions[a]

dye	J_{sc} (mA/cm^2)	V_{oc} (V)	FF	η (%)
D1[b]	10.21	0.70	0.710	5.07
D2[b]	9.56	0.71	0.756	5.13
D3[b]	5.51	0.63	0.726	2.52
D1[c]	10.65	0.72	0.745	5.71
D2[c]	11.62	0.73	0.756	6.41
D3[c]	7.11	0.68	0.747	3.61
N719[d]	15.87	0.71	0.738	8.32

[a] Light source: 100 mW.cm^{-2}, AM 1.5 G simulated solar light; working area: 0.196 cm^2; titania paste was prepared from P25 (Degussa AG, Germany) and added 1% magnesium acetate solution. [b] Dye bath: toluene solution (1×10^{-3} M). [c] Dye bath: toluene solution (1×10^{-3} M) with addition of CDCA (1×10^{-3} M). [d] Dye bath: **N719** in EtOH solution (1×10^{-3} M) with addition of CDCA (1×10^{-3} M).

Photovoltaic Performance of DSSCs Based on the Three Dyes. DSSCs were fabricated using these dyes as the sensitizers, with an effective area of 0.196 cm^2, TiO_2 particles on FTO, and the electrolyte composed of 0.5 M LiI, 0.05 M I_2, and 0.5 M 4-*tert*-butyl-pyridine (TBP) in 3-methoxy-propionitrile. Figure 5 shows incident photon-to-electron conversion efficiency (IPCE) as a function of the wavelength for the sandwiched DSSCs based on the three dyes as sensitizers. The IPCEs action spectra for DSSCs based on **D1** and **D2** are broader than that of **D3**, which is in accordance with their absorption spectra on the transparent TiO_2 films. As shown in Figure 5, the IPCE value of **D3** gives a relatively low value with the maximum of ~33% at 400 nm. The lower IPCE value of the DSSC based on **D3** is probably due to a small energy gap between the LUMO level of the dye and the conduction band edge of TiO_2, which leads to decreased electron injection efficiency relative to those of **D1** and **D2**.[5a] However, the IPCEs action spectra of **D1** and **D2** are very similar but exhibit higher efficiency of ~75% than that of **D3**. The higher IPCE values might attribute to an effective intramolecular cascade energy transfer from di(*p*-tolyl)phenylamine donor to cyanoacetic acid acceptor via Π-spacer.

Under standard global AM 1.5 solar conditions, the **D2**-sensitized cell exhibited better photovoltaic performances (J_{sc} = 9.56 mA/cm^2, V_{oc} = 0.71 V, FF = 0.756, and η = 5.13%) than those of **D1** and **D3**. The power conversion efficiency for the three dyes are in the order of **D3** < **D1** < **D2**, and the corresponding data are 2.52%, 5.07%, and 5.13% (see Table 3). According to the data, it is clear that the efficiencies of the DSSCs can be strongly affected by the electron donor and the hexyl chain in the dye molecules. In comparison to **D3**, the J_{sc}, V_{oc}, and η of **D1** and **D2** are all significantly improved by introducing two di(*p*-toyl)phenylamine groups to form the branchlike configuration. The increased J_{sc} values can be reflected in their high extinction coefficients and the high maximum IPCEs values of **D1** and **D2**. The remarkably increased V_{oc} values of **D1** and **D2** compared with **D3** could be attributed to the effective retardation of charge recombination between the electrons at the TiO_2 and the oxidized dyes (as is shown in Figure 7), which resulted from double di(*p*-tolyl)phenylamine-substitutes or/and hexyl-substitutes in the dyes **D1** and **D2**.[22,13b] In addition, less efficient light harvesting capability of **D2** (i.e., lower high extinction coefficient and less coverage of the IPCEs) likely results in a lower J_{sc} value compared with that of **D1**, but the higher V_{oc} (0.71 V) and FF (0.756) for the device of **D2** might be responsible for their close efficiency between **D1** and **D2**. The slightly higher V_{oc} of **D2** than that of **D1** might be due to the presence of the hexyl chain in **D2**. A long alkyl chain in the thiophene ring can suppress the dye aggregate on TiO_2 surface and reduce charge recombination by preventing the approach of acceptors (i.e., I_3^- ions) to the TiO_2.[22]

To further optimize, CDCA was added into the dye bath, giving much higher photovoltaic performance for the three dyes. The detailed cell performance parameters are compiled in Table 3. The corresponding *J-V* characteristics of DSSCs based on these dyes are shown in Figure 6. The **D2**-sensitized cell exhibited the best photovoltaic performances (J_{sc} = 11.62 mA/cm^2, V_{oc} = 0.73 V, FF = 0.756, and η = 6.41%). The J_{sc} values for DSSCs based on **D2** before and after the addition of CDCA clearly increased from 9.56 mA/cm^2 to 11.62 mA/cm^2, indicating the strong aggregations were effectively suppressed by adding CDCA. For comparison, the η value of DSSCs based on the standard **N719** dye is 8.32% (J_{sc} = 15.87 mA/cm^2, V_{oc} = 0.71 V, FF = 0.738) measured under the same conditions. The result suggests that dye **D2** is a promising metal-free sensitizer in DSSCs.

Transient Absorption Measurements of the Three Dyes on TiO_2 films. Transient absorption spectroscopy was employed to monitor interfacial charge-recombination kinetics in dye sensitized TiO_2 films following laser optical excitation. Details of the transient absorption apparatus have been described previously.[23] This experiment employed low excitation energy densities (≈25 μJ cm^{-2} at 430 nm for all three dyes), these excitation densities being selected to ensure matched densities of absorbed photons for the three dyes, this corresponding to approximately 0.5 injected electron per TiO_2 particle. Considering that the different absorption spectra for these oxidized dyes (as is shown in Figure S3) were recorded and showed a large

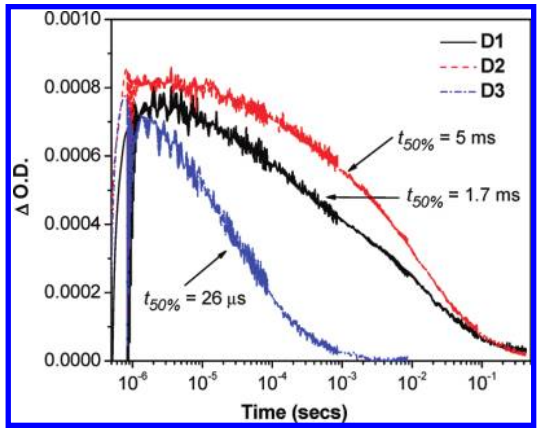

Figure 7. Recombination kinetics of the three dyes on 4 μm TiO_2 covered in propylene carbonate and a transparent cover slide. The kinetics were recorded at 900 nm following excitation at 430 nm.

signal at 900 nm. The typical transient absorption kinetics data were measured by employing a probe wavelength of 900 nm for all samples.

All three dyes show stretched exponential decay kinetics, which has been commonly observed previously in other recombination studies of dye sensitized TiO_2. As is shown in Figure 7, the faster decay kinetics of **D3** ($t_{50\%} = 26$ μs) compared to either **D1** or **D2** ($t_{50\%} = 1.7$ and 5 ms, respectively) can be ascribed to the differences in molecular structure of the dyes. The HOMO of **D1** and **D2** can be expected to be located on two di(*p*-tolyl)phenylamine groups which should be orientated away from the TiO_2 surface. However, **D3** is considerably smaller than **D1** or **D2** and without the presence of any electron-donating di(*p*-tolyl)phenylamine groups, its HOMO will certainly be located closer to the TiO_2 surface, resulting in faster recombination due to smaller distance between charge separated species. All these results strongly support our conclusion that double di(*p*-tolyl)phenylamine-substitutes and hexyl-substitutes in the dyes can increasingly suppressed charge recombination between the electrons at the TiO_2 and the oxidized dyes, which is reflected in the increased V_{oc} and over all device performance above.

Conclusions

In summary, two novel branchlike organic dyes with two di(*p*-tolyl)phenylamine moieties as the electron donor and cyanoacrylic acid as the electron acceptor have been synthesized. It was found that the introduction of two di(*p*-tolyl)phenylamine donors achieved better photovoltaic performances over the dye **D3**. It might be a promising way to suppress aggregation between molecules and enhance the electron-donating ability. The introduction of two di(*p*-tolyl)phenylamine-substitutes as the donors in the molecular structure not only can give obvious blue shifts of UV−vis absorption and emission spectra but also significantly improve the molar extinction coefficients of dyes. The transient absorption measurements showed that di(*p*-tolyl)phenylamine-substitutes and hexyl-substitutes in the dyes can effectively retard charge recombination between the electrons at the TiO_2 and the oxidized dyes. Although the three dyes have relatively narrow absorption spectra, a DSSC based on the high molar extinction coefficient dye **D2** exhibited the optimal η of 6.41% ($J_{sc} = 11.62$ mA/cm^2, $V_{oc} = 0.73$ V, FF = 0.756) by adding the coabsorbent CDCA. The high conversion efficiency reveals that these branchlike organic dyes are promising in the development of DSSCs. Work on further broadening the absorption spectrum for enhancing the light harvesting ability through extending the Π-conjugation system based on these dyes are under study.

Acknowledgment. This work was supported by the National Nature Science Foundation of China (Nos. 50973092), the Nature Science Foundation (Nos. 09JJ3020), and key project (Nos. 2008FJ2004) of Hunan Province of China. The authors are grateful to Prof. Xueye Wang for calculating the molecular modeling. E.P., J.C., and A.F. acknowledge the MICINN for the projects CONSOLIDER (HOPE-0007-2007) and CTQ2007-60746. J.C. also thanks the MICINN for the Juan de la Cierva fellowship.

Supporting Information Available: Experimental details and additional data. This material is available free of charge via the Internet at http://pubs.acs.org.

References and Notes

(1) O'Regan, B.; Grätzel, M. *Nature* **1991**, *353*, 737.

(2) (a) Hauch, A.; Georg, A. *Electrochim. Acta* **2001**, *46*, 3457. (b) Kumar, R.; Sharma, A. K.; Parmar, V. S.; Watterson, A. C.; Chittibabu, K. G.; Kumar, J.; Samuelson, L. A. *Chem. Mater.* **2004**, *16*, 4841. (c) Zhang, D. S.; Downing, J. A.; Knorr, F. J.; McHale, J. L. *J. Phys. Chem. B* **2006**, *110*, 21890. (d) Robertson, N. *Angew. Chem., Int. Ed.* **2006**, *45*, 2338.

(3) Gao, F.; Wang, Y.; Shi, D.; Zhang, J.; Wang, M.; Jing, X.; Humphry-Baker, R.; Wang, P.; Zakeeruddin, S. M.; Grätzel, M. *J. Am. Chem. Soc.* **2008**, *130*, 10720.

(4) (a) Hara, K.; Dan-oh, Y.; Kasada, C.; Ohga, Y.; Shinpo, A.; Suga, S.; Sayama, K.; Arakawa, H. *Langmuir* **2004**, *20*, 4205. (b) Wang, Z.-S.; Cui, Y.; Hara, K.; Dan-oh, Y.; Kasada, C.; Shinpo, A. *Adv. Mater.* **2007**, *19*, 1138.

(5) (a) Ito, S.; Zakeeruddin, S. M.; Humphrey-Baker, R.; Liska, P.; Charvet, R.; Comte, P.; Nazeeruddin, M. K.; Péchy, P.; Takata, M.; Miura, H.; Uchida, S.; Grätzel, M. *Adv. Mater.* **2006**, *18*, 1202. (b) Horiuchi, T.; Miura, H.; Sumioka, K.; Uchida, S. *J. Am. Chem. Soc.* **2004**, *126*, 12218. (c) Snaith, H. J.; Petrozza, A.; Ito, S.; Miura, H.; Grätzel, M. *Adv. Funct. Mater.* **2009**, *19*, 1810.

(6) (a) Kitamura, T.; Ikeda, M.; Shigaki, K.; Inoue, T.; Anderson, N. A.; Ai, X.; Lian, T.; Yanagida, S. *Chem. Mater.* **2004**, *16*, 1806. (b) Hara, K.; Sato, T.; Katoh, R.; Furube, A.; Yoshihara, T.; Murai, M.; Kurashige, M.; Ito, S.; Shinpo, A.; Suga, S.; Arakawa, H. *Adv. Funct. Mater.* **2005**, *15*, 246.

(7) (a) Sayama, K.; Tsukagoshi, S.; Hara, K.; Ohga, Y.; Shinpou, A.; Abe, Y.; Suga, S.; Arakawa, H. *J. Phys. Chem. B* **2002**, *106*, 1363. (b) Sayama, K.; Hara, K.; Mori, N.; Satsuki, M.; Suga, S.; Tsukagoshi, S.; Abe, Y.; Sugihara, H.; Arakawa, H. *Chem. Commun.* **2000**, 1173.

(8) (a) Wang, Z.-S.; Li, F.-Y.; Huang, C.-H. *Chem. Commun.* **2000**, 2063. (b) Yao, Q.-H.; Shan, L.; Li, F.-Y.; Yin, D.-D.; Huang, C.-H. *New J. Chem.* **2003**, *27*, 1277.

(9) (a) Campbell, W. M.; Jolley, K. W.; Wagner, P.; Wagner, K.; Walsh, P. J.; Gordon, K. C.; Schmidt-Mende, L.; Nazeeruddin, M. K.; Wang, Q.; Grätzel, M; Officer, D. L. *J. Phys. Chem. C* **2007**, *111*, 11760. (b) Liu, Y.-J.; Xiang, N.; Feng, X.-M.; Shen, P.; Zhou, W.-P.; Weng, C.; Zhao, B.; Tan, S.-T. *Chem. Commun.* **2009**, *18*, 2499.

(10) (a) Li, G.; Jiang, K.-J.; Li, Y.-F.; Li, S.-L.; Yang, L.-M. *J. Phys. Chem. C* **2008**, *112*, 11591. (b) Thomas, K. R. J.; Hsu, Y.-C.; Lin, J. T.; Lee, K.-M.; Ho, K.-C.; Lai, C.-H.; Cheng, Y.-M.; Chou, P.-T. *Chem. Mater.* **2008**, *20*, 1830. (c) Hagberg, D. P.; Yum, J.-H.; Lee, H.; De Angelis, F.; Marinado, T.; Karlsson, K. M.; Humphry-Baker, R.; Sun, L.; Hagfeldt, A.; Grätzel, M.; Nazeeruddin, M. K. *J. Am. Chem. Soc.* **2008**, *130*, 6259. (d) Tsai, M.-S.; Hsu, Y.-C.; Lin, J.-T.; Chen, H.-C.; Hsu, C.-P. *J. Phys. Chem. C* **2007**, *111*, 18785. (e) Zhang, G.-L.; Bala, H.; Cheng, Y.-M.; Shi, D.; Lv, X.-J.; Yu, Q.-J.; Wang, P. *Chem. Commun.* **2009**, 2198.

(11) (a) Koumura, N.; Wang, Z.-S.; Mori, S.; Miyashita, M.; Suzuki, E.; Hara, K. *J. Am. Chem. Soc.* **2006**, *128*, 14256. (b) Wang, Z.-S.; Koumura, N.; Cui, Y.; Takahashi, M.; Sekiguchi, H.; Mori, A.; Kubo, T.; Furube, A.; Hara, K. *Chem. Mater.* **2008**, *20*, 3993.

(12) (a) Ning, Z.-J.; Zhang, Q.; Wu, W.-J.; Pei, H.-C.; Liu, B.; Tian, H. *J. Org. Chem.* **2008**, *73*, 3791. (b) Yum, J.-H.; Jung, I. L.; Baik, C.; Ko, J.; Nazeeruddin, M. K.; Grätzel, M. *Energy Environ. Sci.* **2009**, *2*, 100.

(13) (a) Haque, S. A.; Handa, S.; Peter, K.; Palomares, E.; Thelakkat, M.; Durrant, J. R. *Angew. Chem., Int. Ed.* **2005**, *44*, 5740. (b) Karthikeyan, C. S.; Wietasch, H.; Thelakkat, M. *Adv. Mater.* **2007**, *19*, 1091.

(14) Bonhote, P.; Moser, J.-E.; Humphry-Baker, R.; Vlachopoulos, N.; Zakeeruddin, S. M.; Walder, L.; Gräztzel, M. *J. Am. Chem. Soc.* **1999**, *121*, 1324.

(15) Hagberg, D. P.; Edvinsson, T.; Marinado, T.; Boschloo, G.; Hagfeldt, A.; Sun, L. *Chem. Commun.* **2006**, 2245.

(16) Nazeeruddin, M. K.; Kay, A.; Rodicio, I.; Humphry-Baker, R.; Müller, E.; Liska, P.; Vlachopoulos, N.; Grätzel, M. *J. Am. Chem. Soc.* **1993**, *115*, 6382.

(17) Kumara, G. R. A.; Kaneko, S.; Konno, A.; Okuya, M.; Murakami, K.; Onwona-agyeman, B.; Tennakone, K. *Prog. Photovolt: Res. Appl.* **2006**, *14*, 643.

(18) Chen, R.-k.; Yang, X.-C.; Tian, H.-N.; Wang, X.-N.; Hagfeldt, A.; Sun, L.-C. *Chem. Mater.* **2007**, *19*, 4007.

(19) Demandrille, R.; Firon, M.; Leroy, J.; Rannou, P.; Pron, A. *Adv. Funct. Mater.* **2006**, *16*, 1694.

(20) Roquet, S.; Cravino, A.; Leriche, P.; Alévêque, O.; Frère, P.; Roncali, J. *J. Am. Chem. Soc.* **2006**, *128*, 3459.

(21) Hara, K.; Sato, T.; Katoh, R.; Furube, A.; Ohga, Y.; Shinpo, A.; Suga, S.; Sayama, K.; Sugihara, H.; Arakawa, H. *J. Phys. Chem. B* **2003**, *107*, 597.

(22) (a) Schmidt-Mende, L.; Kroeze, J. E.; Durrant, J. R.; Nazeeruddin, M. K.; Grätzel, M. *Nano Lett.* **2005**, *5*, 1315. (b) Kroeze, J. E.; Hirata, N.; Koops, S.; Nazeeruddin, M. K.; Schmidt-Mende, L.; Grätzel, M.; Durrant, J. R. *J. Am. Chem. Soc.* **2006**, *128*, 16376.

(23) (a) Haque, S. A.; Tachibana, Y.; Willis, R. L.; Moser, J. E.; Grätzel, M.; Klug, D. R.; Durrant, J. R. *J. Phys. Chem. B* **2000**, *104*, 538. (b) Palomares, E.; Clifford, J. N.; Haque, S. A.; Lutz, T.; Durrant, J. R. *J. Am. Chem. Soc.* **2003**, *125*, 475. (c) Haque, S. A.; Park, T.; Xu, C.; Koops, S.; Schultes, N.; Potter, R. J.; Holmes, A. B.; Durrant, J. R. *Adv. Funct. Mater.* **2004**, *14*, 435. (d) Cíd, J. J.; García-Iglesias, M.; Yum, J. H.; Forneli, A.; Albero, J.; MartÍnez-Ferrero, E.; Vázquez, P.; Grätzel, M.; Nazeeruddin, M. K.; Palomares, E.; Torres, T. *Chem.—Eur. J.* **2009**, *15*, 5130.

JP911139X